JOURNAL OF PROPULSION AND POWER
Vol. 8, No. 6, Nov.–Dec. 1992

Mixing and Combustion Studies Using Discrete Orifice Injection at Hypervelocity Flight Conditions

R. Bakos,* J. Tamagno,† R. Trucco,‡ O. Rizkalla,§ W. Chinitz,¶ and J. I. Erdos**
General Applied Science Laboratories, Inc., Ronkonkoma, New York 11779

A Mach 13 operating point was achieved in the HYpersonic PULSE facility (HYPULSE) expansion tube and hydrogen injection studies were performed at this test condition. The experiments were conducted in a 2- × 1-in. combustor model employing three injector configurations: 1) a single, flush-wall, circular orifice; 2) two such orifices on opposite walls (the "dual" injector configuration); and 3) two orifices on the upper and lower walls (the "quad" injector configuration). The quad injectors were distinctly superior to the other two configurations in promoting mixing, ignition, and combustion. The single injector, however, proved to be superior to the dual injectors, supporting the concept that the aspect ratio of the "injection cell" plays a large role in promoting the processes required to achieve high-combustion efficiency.

Nomenclature

A^*	=	injector throat area
a, b	=	curve-fit coefficients in Eq. (1)
C_d	=	injector-discharge coefficient
H	=	total (stagnation) enthalpy
h	=	injection cell height
M	=	Mach number
P	=	pressure
$\dot{q}$	=	heat flux
Re_{tr}	=	transition Reynolds number
St	=	modified Stanton number
T	=	temperature
u	=	velocity
x	=	axial distance
η_c	=	combustion efficiency
ρ	=	mass density
ϕ	=	fuel-oxidizer equivalence ratio

Subscripts

comb, combustion	=	combustion test-run
IN, inlet	=	combustor model inlet
inj	=	fuel injector state
mix, mixing	=	mixing test-run
s, static	=	static state
t	=	total (stagnation) state
2	=	pitot state
∞	=	flight conditions

I. Introduction

EFFICIENT combustion in a scramjet engine requires a fuel injection system which achieves full mixing of the fuel and air within the limited combustor length. This mixing process can be thought of as occurring in two steps. The first is the initial pressure and direction-matching of the injected fuel steams with the combustor airflow. This process is not truly a mixing process since it occurs nearly inviscidly; however, it is important because it determines the initial distribution of fuel over the combustor cross section. For this step to be effective, the fuel streams must be evenly distributed, either by the use of an instream-injection device or by imparting sufficient crossflow momentum to a wall jet so as to propel it across the duct. Another alternative is to create large-scale turbulent motions (by means of a vortex-generating device) in the airstream to mix the fuel and air downstream of injection. The second step is the small-scale turbulent mixing which occurs at the interface that exists between the injected fuel streams and the air. It is this process which achieves the micromixing necessary for chemical reaction to occur. The dependence of the efficiency of this second process on the details of the initial fuel injection geometry is not clear. Intuitively, one might anticipate that these processes become less effective at the higher flight Mach numbers when the diffusive spread-rate of the fuel becomes small relative to the rate at which air sweeps through the combustor. Therefore, testing of injection configurations at the higher flight speeds is of utmost importance for developing a successful flight system.

There exist numerous choices for the injector design; however, injection from a number of transverse wall jets may prove to be a very simple and desirable solution, if such a design can be shown to achieve the necessary cross-stream penetration and downstream mixing. Previous investigations at high-flight Mach numbers (Ref. 1) have shown that the number, size, and spacing of the jets has a distinct effect on the measured combustor performance, and therefore, on the extent of mixing. Equally important, however, is the injection angle with respect to the freestream direction. Intuitively, injecting normal to the combustor wall would maximize the fuel cross-stream momentum, and therefore, be most effective at fueling the entire duct. However, at high-flight Mach numbers, a significant portion of the net thrust produced by a scramjet results from the streamwise component of the fuel momentum. Therefore, a tradeoff in fuel penetration must be made to retain an axial momentum component of the fuel.

It is the objective of this effort to experimentally determine the effects of several flush-wall-injection design parameters on scramjet combustor performance at Mach 13.5 flight conditions. Tests were conducted in a rectangular combustor model fueled by one, two, and four transverse wall jets. The test conditions simulating the Mach 13.5 flight condition were produced in the HYPULSE facility expansion tube. The operational capabilities of this facility (in its current configuration) were discussed in Refs. 2 and 3, as were the details of expansion tube operation.

Presented as Paper 91-2396 at the AIAA/ASME/SAE/ASEE 27th Joint Propulsion Conference, Sacramento, CA, June 24–26, 1991; received July 15, 1991; revision received March 17, 1992; accepted for publication April 21, 1992.

*Senior Scientist. Member AIAA.
†Principal Scientist. Member AIAA.
‡Scientist.
§Scientist. Member AIAA.
¶Principal Scientist; also, Professor of Mechanical Engineering, Cooper Union, Nerken School of Engineering. Associate Fellow AIAA.
**Vice President. Associate Fellow AIAA.

II. Mach 13 Facility Calibration

An extensive facility calibration for the Mach 13 test condition was recently completed. The data are highly repeatable and are sufficient to delineate this test condition with a high degree of confidence. Figure 1 shows the radial distribution of pitot-to-static pressure at the entrance to the test chamber as obtained from a pitot-static pressure rake. As can be seen, a uniform core exists over the central 1.5–2 in. of the flow captured by the combustor models. Figure 2, which shows static pressure and Mach number time histories at the acceleration tube exit, reveals that the former increases slightly with time while the latter slightly decreases. This temporal behavior may be due to the arrival of a weak wave system associated with the growth of the boundary layer along the tube wall.

For the tests described here, the period from 400 to 800 μs after shock arrival is regarded as steady, useful test time. It should be noted in Fig. 2 that the passage of the acceleration gas requires about 150 μs, after which the test gas arrives and stabilizes during the next 250 μs. In addition, although the initial 400 μs are not considered to be part of the useful test time, they do contribute to the establishment of flow in the model.

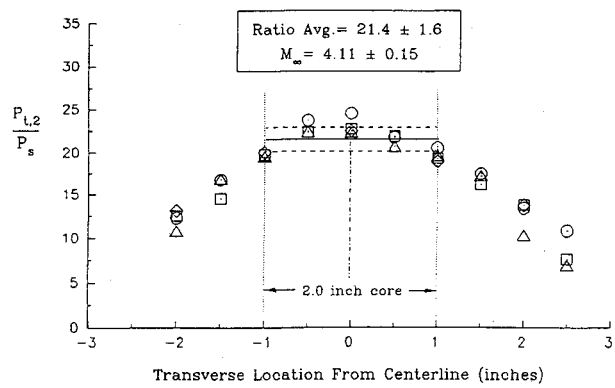

Fig. 1 Pitot-to-static pressure ratio at the exit of the acceleration chamber (air-test gas; 5500 psi driver pressure).

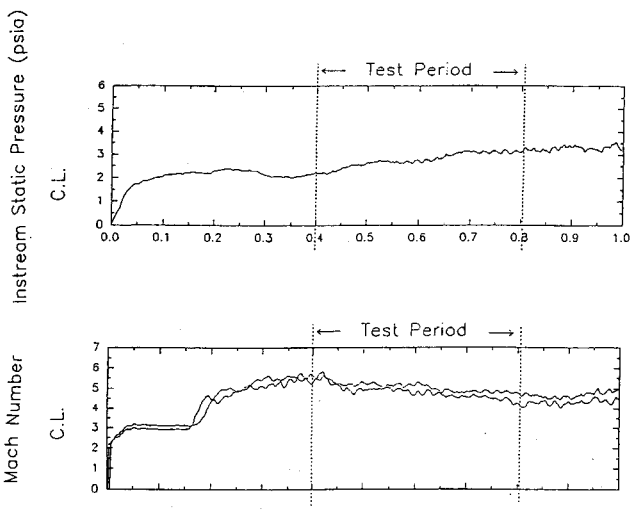

Fig. 2 Instream static pressure and Mach number as functions of time at three radial locations in the exit plane.

Table 1 Air properties at the Mach 13 test condition

	SI	ENGRG
Velocity	3,840 m/s	12,600 ft/s
Static pressure	18,197 Pa	2.64 psia
Static temperature	2,350 K	4,230 R
Mach number	4.11	4.11
Total pressure	10,491 kPa	1,522 psia
Total temperature	5,788 K	10,400 R
Post normal shock conditions		
Total pressure	390 kPa	56.6 psia
Total temperature	5,162 K	9,292 R

Table 1 summarizes the measured and derived test conditions at the Mach 13 test condition. The methods of Mirels[4] were used to derive the gas velocity from the measured shock speed.

III. Combustor Model

The 2-in. (0.0508-m) by 1-in. (0.0254-m) cross-section combustor model, which is 28-in. long (0.711-m), is shown in Fig. 3. The leading edges are sharp wedges having a tip bluntness of 0.020-in. (5.08×10^{-4} m) nominal diam. Optical-quality windows in the model side walls permit flow visualization extending from the 3.25-in. (0.08255-m) to the 15.25-in. (0.38735-m) model stations.

Fuel injection manifold plates are located on the upper and lower walls. Changes in fuel injector configuration are made by changing these plates. The manifolds are each supplied by the Ludweig tube system described in Ref. 3. Fuel injection conditions are summarized in Table 2. Instrumentation consists of wall static pressures and heat flux gauges on the upper and lower model surfaces. A total of 43 instrument ports were located in the model, of which 30 measured pressure and 13 measured wall heat flux.

IV. Experimental Results

A principal objective of the initial test series using the rectangular combustor model was to determine the influence of different injector geometries on ignition and combustion. The three injector configurations, consisting of one, two, and four injectors, are shown schematically in Fig. 4. Testing was performed at a fuel-air equivalence ratio of 2.6, the fuel-exit Mach number from the circular orifices in all cases was 1, the injection angle of the fuel was 30 deg from the freestream direction, and the total injector area was held constant for the three cases. To accurately set injection mass flow rates, the effective throat area C_dA^*, was determined by calibration for each configuration.

The test procedure consisted of three types of test runs: 1) fuel-off runs intended to characterize the effects of the wall boundary layer on the flow through the model ("tare runs"); 2) tests with hydrogen injection into nitrogen to superimpose the additional influence of the mixing process on the measurable parameters ("mixing runs"); and 3) full combustion tests with hydrogen injected into air, thereby incorporating the additional effects of chemical reaction on the flow processes ("combustion runs"). Differences among these types of runs were interpreted as being solely the result of the different identifiable processes, i.e., viscous, mass addition (mixing), and combustion, respectively.

A. Data Acquisition and Reduction

The short steady flow period in the HYPULSE facility requires high-data sampling rates. To this end the data were sampled at 500 KHz, thus providing approximately 200 data samples within the 400 μs of test time.

Table 2 Fuel injector conditions

Injector configuration	C_dA^*, in.^{2}	Test gas	Fuel P_t, psia	Equivalence ratio, approx.
Single	0.0273	N_2	124.5	2.40
Single		Air	123.6	2.38
Dual	0.0244	N_2	151.6	2.61
Dual		Air	153.1	2.64
Quad	0.0235	N_2	162.0	2.69
Quad		Air	162.4	2.69
Quad		O_2	163.0	2.70
T_t = 300 K				
M_{inj} = 1				

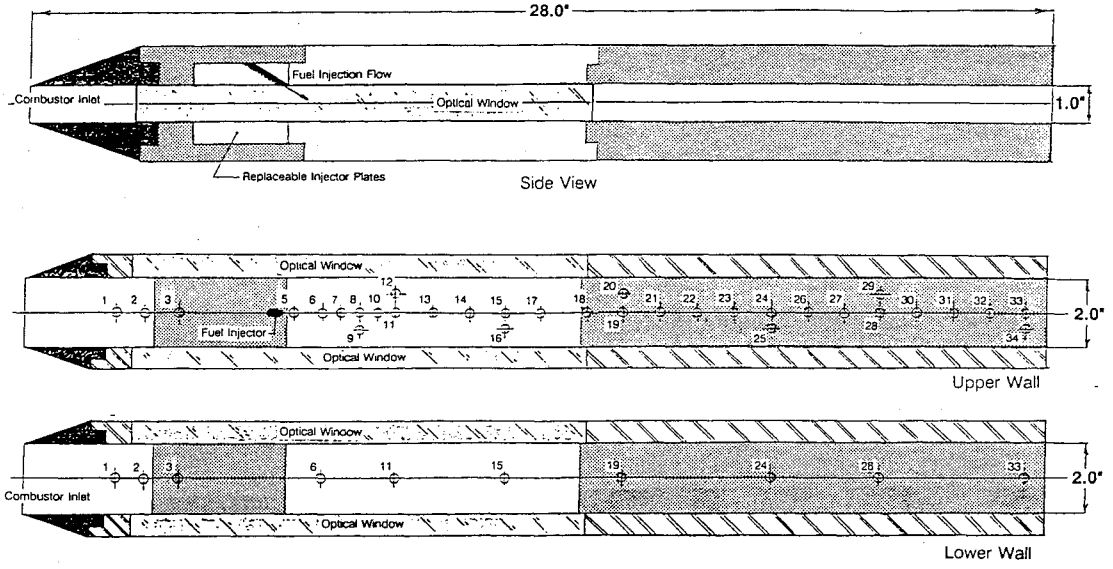

Fig. 3 Rectangular combustor model.

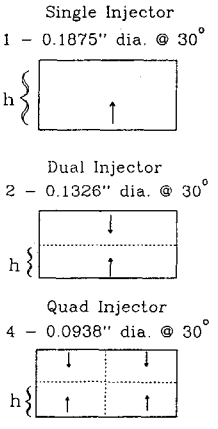

Fig. 4 Schematic of the single-, dual-, and quad-injector configurations.

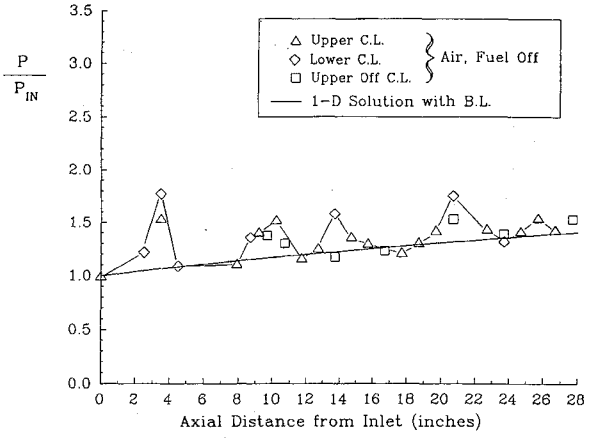

Fig. 5 Tare-run static pressure distribution (air-test gas).

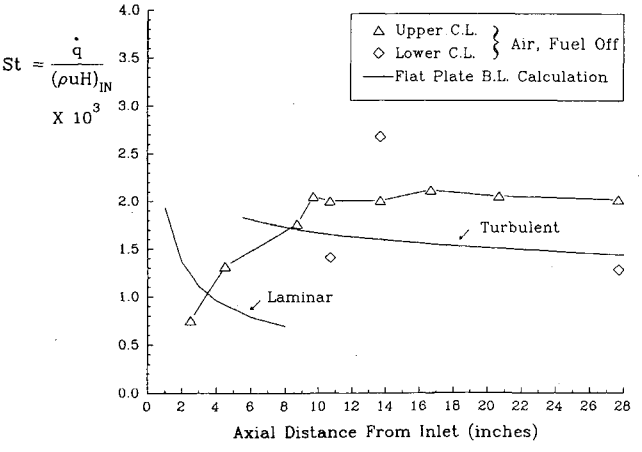

Fig. 6 Tare-run heat flux distribution (air-test gas).

Within the facility test period the combustor flow must also relax to a steady state, and a consistent methodology for detecting and obtaining steady flow combustor data is required to achieve repeatable and reliable results. As discussed previously, the sequence of flow events within the model begins with the facility starting shock, followed in approximately 400 μs by the start of the test time. In approximately another 100 μs, the static pressure and heat transfer in the model achieve steady values and remain approximately constant for the remaining 300 μs of the test period. During this final 300 μs the data is time-averaged to obtain the steady pressure and heat flux values reported.

B. Injector Configuration Experiments

Figure 5 shows the measured distribution of static pressure for the fuel-off tare run with air-test gas and Figs. 7a–f show pressures for the three injector configurations tested with both nitrogen and air-test gases. Repeated on each plot is the tare-run pressure distribution so that the effects of fuel addition and combustion can be clearly seen. Corresponding wall heat flux data are shown in Fig. 6 and Figs. 8a–f, again plotted with the fuel-off data on each plot for reference.

Note that to detect gradients in the cross-stream directions, transducers were placed on both the upper (injection side for single-injector case) surface and lower surface centerlines, as well as 0.5 in. off the upper surface centerline. In each plot the centerline data points have been connected to give a feel for the overall trends with axial distance.

Considering the tare run (Fig. 5), the high pressure measured at the 3.5-in. station is a result of the shock generated at the model leading edge which reflects back to the wall from the symmetry plane. The strength of this shock is dictated by the combined effects of viscous interaction and a leading-edge bluntness of 0.020 in. This standing wave system persists through the duct and is modulated by an underlying pressure increase with distance resulting from viscous drag. Also shown is a pressure distribution computed by integration of the one-dimensional equations of motion for the closed duct. The

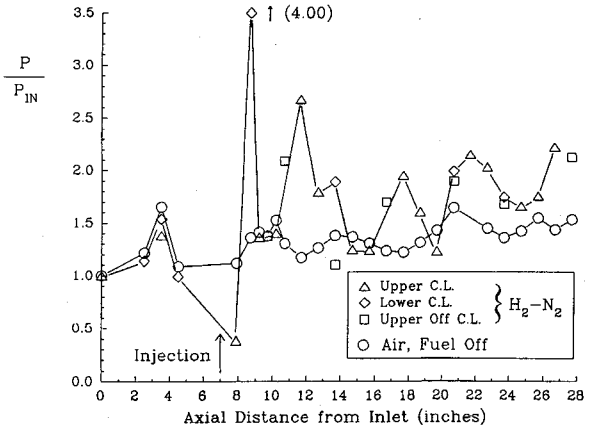

a) Single-injector mixing run

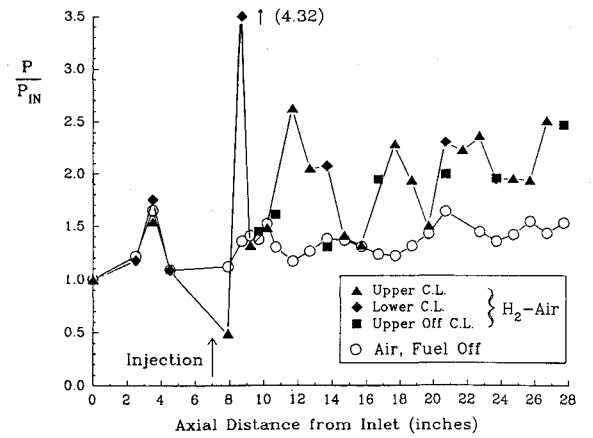

b) Single-injector combustion run

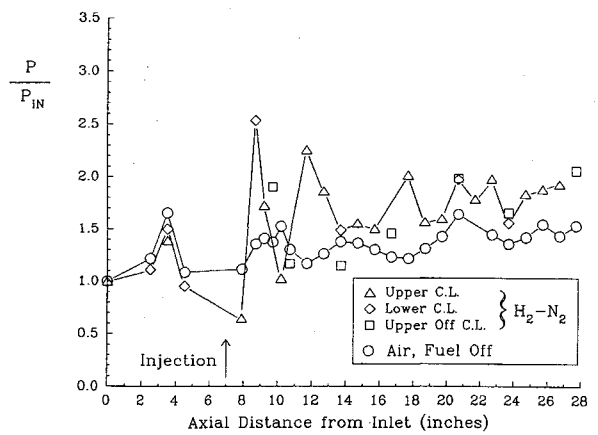

c) Dual-injector mixing run

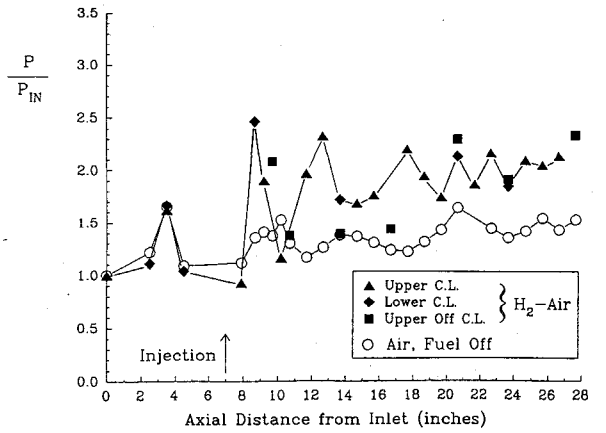

d) Dual-injector combustion run

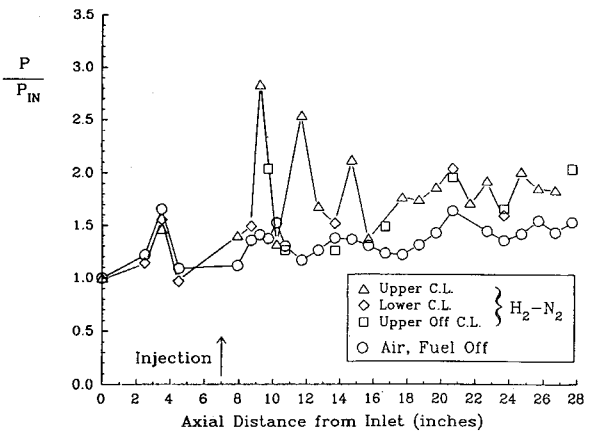

e) Quad-injector mixing run

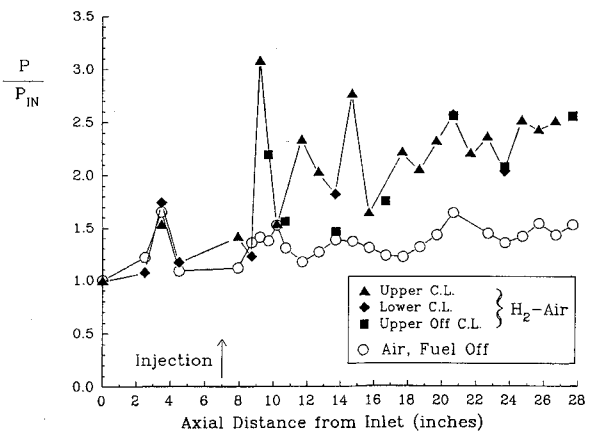

f) Quad-injector combustion run

Fig. 7 Axial pressure distribution with hydrogen injection.

effects of momentum loss due to wall shear and energy loss due to wall heat transfer are included by way of a formula for skin friction in a zero-pressure gradient compressible flow[5] and Reynolds analogy for heat transfer. The mean pressure distribution trend, excluding the wave structure since this is a one-dimensional calculation, is seen to be slightly underpredicted because of the exclusion of the oblique shock losses.

The computed Stanton number distribution is plotted in Fig. 6 with the corresponding tare-run data. Recognizing that the scatter of the lower centerline points probably results from a calibration error, reasonable agreement is seen in the aft portion of the duct. The limited spatial resolution of the measurements does not permit clear identification of the laminar-turbulent transition location. However, at least the first several inches may be laminar as can be seen by comparison with a theoretical curve for laminar heat flux as computed by the Eckert reference enthalpy method. Note that with transition beginning at $x = 6.0$ in., a value of $Re_{tr}/M = 75$ is computed, well below the accepted range of 150–300 for flight. It is difficult to unequivocally determine the cause of this early transition; however, the facility turbulence level at this particular operating condition is known to be high, as evidenced by the fluctuations in the exit plane Mach number traces (Fig. 2) and the existence of a turbulent boundary layer on the acceleration tube wall at this condition, as evidenced by facility heat transfer measurements. Furthermore, the leading-

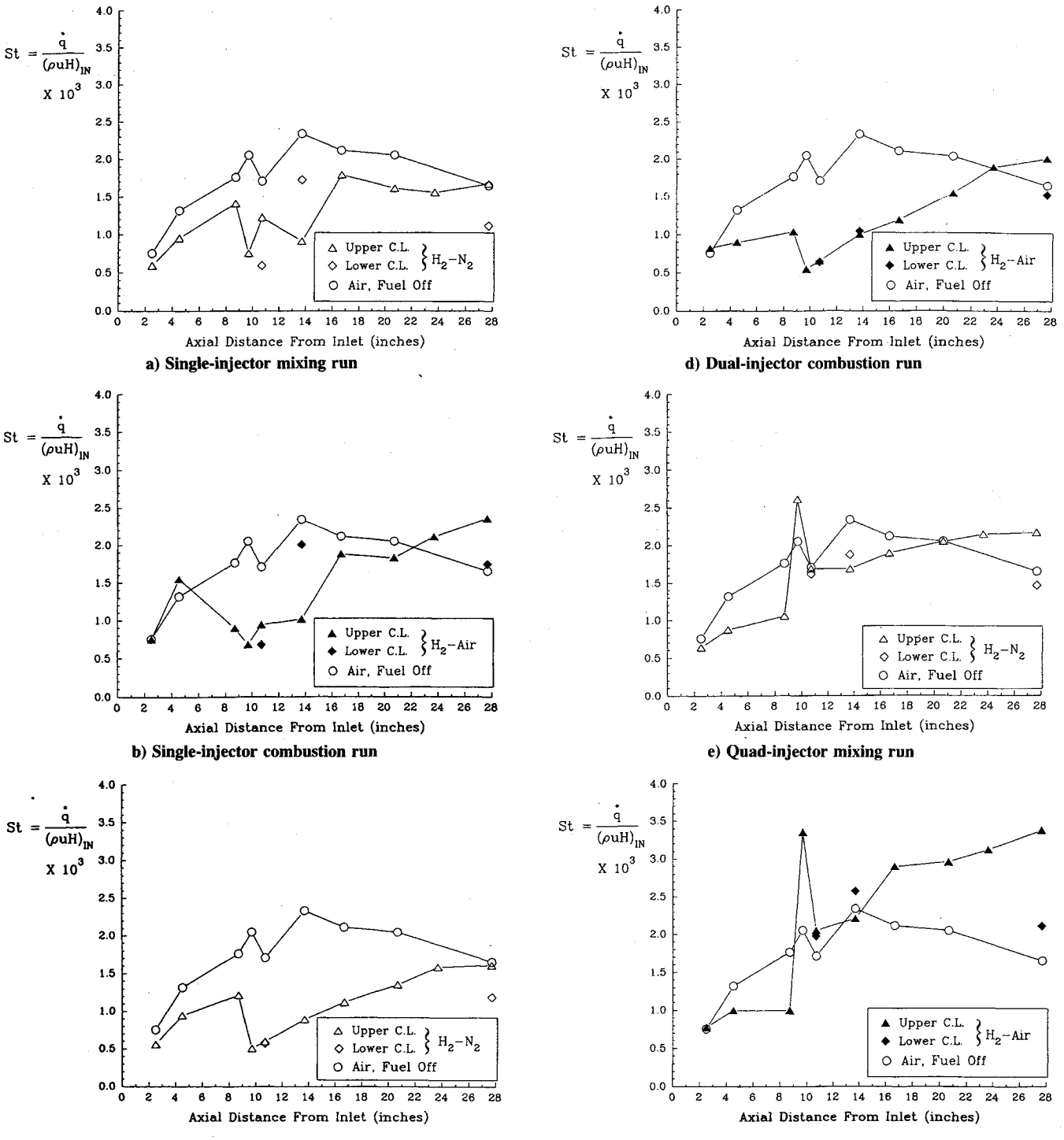

a) Single-injector mixing run

b) Single-injector combustion run

c) Dual-injector mixing run

d) Dual-injector combustion run

e) Quad-injector mixing run

f) Quad-injector combustion run

Fig. 8 Axial heat flux distribution with hydrogen injection.

edge shock system clearly disrupts the boundary layer and may serve as an effective trip device.

Pressure distributions for the single-orifice configuration are shown in Figs. 7a and 7b. Upstream of the injector location the pressures are nearly identical to the tare data. Considerable upper-lower asymmetry is seen for this case; however, gradients in the third cross-stream dimension were found to be minor. A pronounced wave structure is generated by the fuel addition with the injector bow shock reflecting off the lower wall, as indicated by the high pressure recorded at the 8.7-in. transducer station. Comparison of the mixing and combustion data suggests that some pressure-rise due to heat release was achieved.

The heat flux distributions in Figs. 8a and 8b show some film-cooling effect on the upper (injection) surface when compared with the tare run. A small additional increment in heat flux is seen for the combustion case approaching the duct exit.

The dual injector pressure data in Figs. 7c and 7d show a less intense wave structure when compared with the single injector. Again, the pressure rise achieved due to heat release is small. This may be explained by considering the heat flux data in Figs. 8c and 8d. There is a noticeable film-cooling effect over the entire duct length indicating that the fuel does not mix well. The geometry for this case is such that a 4:1 aspect ratio cell needs to be fueled by each injector. This requires considerable lateral spreading, which apparently is not achieved.

Comparing the quad-injector pressure distributions for mixing and combustion (Figs. 7e and 7f) evidence of combustion heat release is clearly seen. The heat flux distributions in Figs.

8e and 8f show no film cooling as is expected with the injectors located off the centerline at ±0.5 in. A local hot-spot is created just downsteam of injection at the 9.7-in. station.

The relative pressure rise achieved by the three configurations are compared in Fig. 9, wherein the normalized pressure difference term

$$\Delta\bar{P} = (P/P_{\text{inlet}})_{\text{combustion}} - (P/P_{\text{inlet}})_{\text{mixing}}$$

is plotted as a function of dimensionless distance x/h, where h is the "gap height" defined in Fig. 4. The curves shown are data regressions of the form

$$\bar{\Delta P} = a\{1-\exp[b(x-x_{\text{injection}})]\} \qquad (1)$$

This normalization procedure correlates the geometrically similar quad and single injectors reasonably well in accordance with the observation that these two configurations involve injection cells having aspect ratios of 2:1. On the other hand, the inability to correlate the dual injector is a consequence of its lack of geometric similarity, since the injection cell aspect ratio is 4:1. These results parallel those in Ref. 1 in which it was concluded that the dimensions of the injection cell determine the rate of downstream mixing. The experiments of Ref. 1 were conducted over a similar range of hypervelocity flow total enthalpies.

C. Oxygen Test Gas Experiments

In its current configuration, the HYPULSE expansion tube may be pressure-limited when conducting some types of combustion experiments. That is, the (air) test gas static pressure may be low enough to result in chemical kinetic limitations on the H_2-air ignition and combustion processes. To circumvent this present limitation, the use of oxygen as a test gas has been found to be an effective means of ensuring complete combustion within the available duct length.

In this connection, an experiment was run using the quad-injector configuration with O_2 as the test gas at (nominally) identical conditions as in air (Table 1) and (nominally) identical fuel flow rate. Figures 10 and 11 show the measured pressure and heat flux distributions for this case. Fig. 12 contrasts the previously-discussed H_2-air case with this H_2-O_2 run. Also shown are the results of premixed, one-dimensional, finite-rate calculations, which neglect skin friction and heat loss at the wall. The chemical kinetic mechanism and associated rate coefficients are from Ref. 6. As can be seen, good agreement is obtained for the H_2-air case, suggesting once again that the quad injector produces mixing efficiencies approaching 100%. It is also clear that since the final equilibrium state has not been reached at the combustor exit, the reaction with air is chemical kinetically-limited at these conditions.

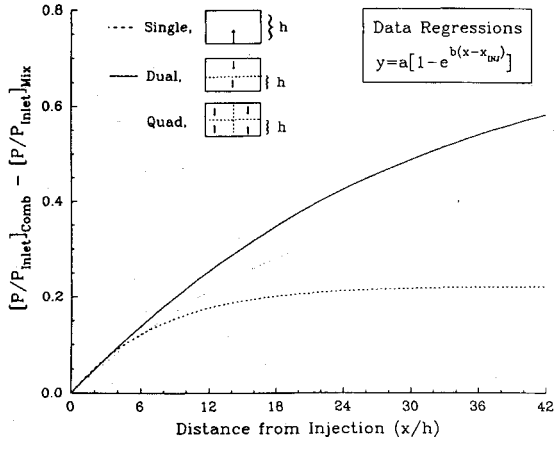

Fig. 9 Effect of length-to-gap height ratio on combustion pressure rise.

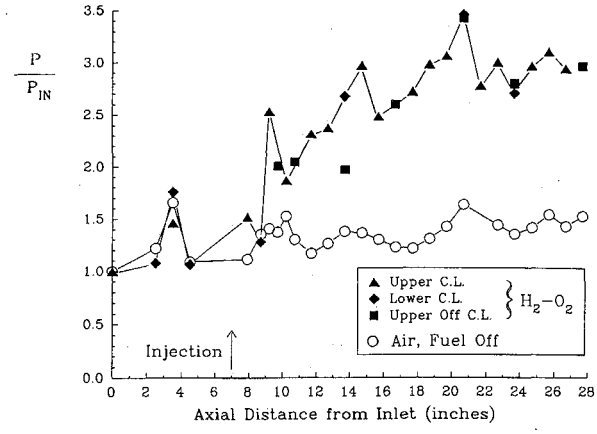

Fig. 10 Axial pressure distribution with hydrogen injection into oxygen test gas.

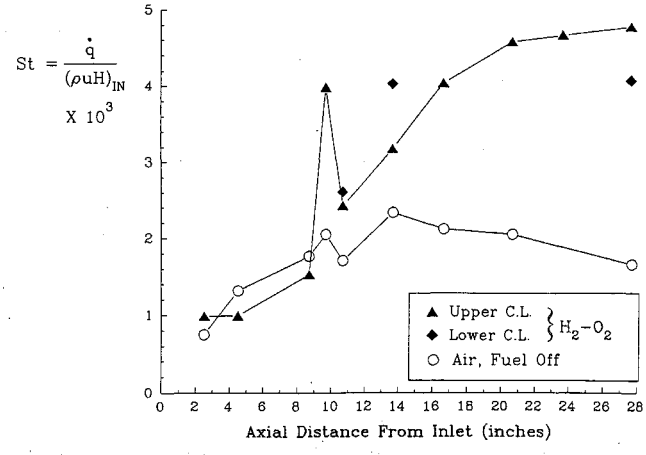

Fig. 11 Axial heat flux distribution with hydrogen injection into oxygen test gas.

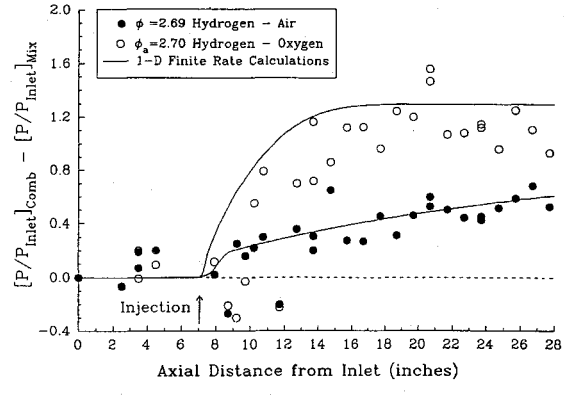

Fig. 12 Comparison between hydrogen combustion in air and in oxygen.

On the other hand, both the experimental data and the calculation for the pure oxygen test indicate that the reaction rate processes have reached equilibrium within about 10 in. of the injection location. It is of interest to note that the equilibrium $\Delta\bar{P}$ value (reached experimentally) is somewhat lower than that indicated by the calculation, which is reflective of the assumptions in the analysis (e.g., adiabatic wall).

V. Combustor Performance Assessments

To develop a basis for comparison of the combustor performance achieved with the different injection schemes, a one-dimensional equilibrium cycle code (Ref. 7) was used. For pulse facility scramjet tests, the most accessible and reliable diagnostic for gauging combustion heat release is the static pressure distribution. However, when testing in the hy-

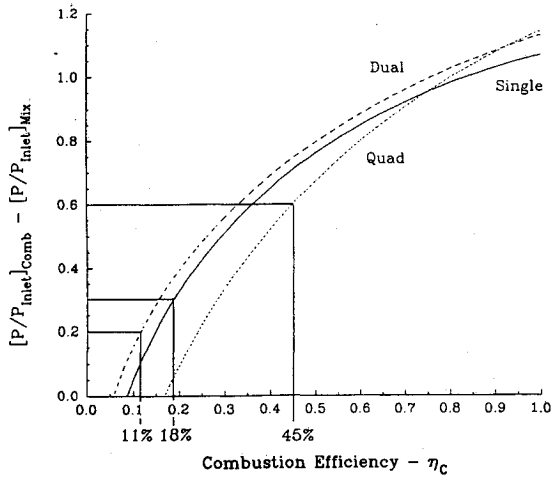

Fig. 13 Predicted combustion pressure rise as a function of combustion efficiency.

pervelocity regime, the effects of skin-friction drag, heat loss to the walls, and injection-shock-induced losses also strongly influence the measured duct static pressure level, making it a less sensitive indicator of performance. Including these effects in an approximate manner is more easily done in a one-dimensional cycle code.

To accomplish this, the cycle code is run in a pressure-predictive manner with the fuel assumed to mix and react instantaneously to equilibrium upon injection. The completeness of the reaction is governed by an input-combustion efficiency. The measured heat flux distribution is also input and a local momentum-loss coefficient was calculated using a local flat-plate skin friction correlation for compressible flow.[5] It is recognized that this flat-plate correlation may not be satisfactory for the nonzero pressure gradient existing in the duct. Therefore, for each injector configuration, a correction factor for the flat-plate momentum loss was chosen so that the pressure rise measured in a mixing run was matched. This same correction factor was then used to predict the pressure rise for parametrically varied combustion efficiencies.

These predictions are summarized in Fig. 13 as the difference between predicted combustor-exit pressures for mixing and combustion runs normalized by the duct inlet pressure and plotted vs combustion efficiency. By also plotting the measured data it is possible to infer the combustion efficiency. It is again clear that of the three injector configurations, the quad injector performed most favorably; however, in no case is complete combustion achieved.

VI. Conclusions

The ability to adjust the HYPULSE expansion tube's operational characteristics to achieve a number of test conditions has been demonstrated by the newly calibrated Mach 13 condition. This, added to the previously obtained Mach 17 test condition, holds the promise of achieving other operating conditions in the hypervelocity regime, thereby substantially increasing the facility's flexibility and utility.

Experiments conducted in the facility using a 2 × 1 in. rectangular combustor model which employed three different hydrogen fuel injector configurations, strongly support the concept that injection cell dimensions play a large role in promoting mixing of the fuel and oxidizer. (Alternatively, as was pointed out by one reviewer, one could say that the mixing is limited to a certain cell size which is dependent upon oxidizer flow conditions and fuel injection conditions.)

Single- and quad-injector configurations, in which the injection cell aspect ratio was 2:1, clearly outperformed a dual-injector configuration having an injection cell aspect ratio of 4:1. Of the former two configurations, the quad injectors were distinctly superior in promoting mixing and subsequent combustion. For example, calculations performed using a one-dimensional, equilibrium chemistry cycle code lead to inferred combustion efficiencies of 18% (single injector), 11% (dual) and 45% (quad).

A comparison between results of quad-injector tests using air and oxygen as test gases, demonstrated that significant chemical kinetic limitations exist when using air. This resulted from the relatively low-static pressure and high-initial temperature at this test condition.

Acknowledgments

This work was sponsored by the NASA Langley Research Center under Contract NAS1-18450 with E. A. Mackley and A. G. McLain serving as Technical Monitors.

References

[1]Morgan, R. G., and Casey, R., "Supersonic Combustion with Transverse Circular Wall Jets," NASA CR-182096, Oct. 1990.

[2]Rizkalla, O., Bakos, R. J., Chinitz, W., Pulsonetti, M. V., and Erdos, J. I., "Use of an Expansion Tube to Examine Scramjet Combustion at Hypersonic Velocities," AIAA Paper 89-2536, Boston, MA, July 1989.

[3]Bakos, R. J., Tamagno, J., Rizkalla, O., Pulsonetti, M. V., Chinitz, W., and Erdos, J. I., "Hypersonic Mixing and Combustion Studies in the GASL HYPULSE Facility," *Journal of Propulsion and Power*, Vol. 8, No. 4, 1992, pp. 900–906.

[4]Mirels, H., "Test Time in Low Pressure Shock Tubes," *Physics of Fluids*, Vol. 6, Sept. 1963, pp. 1202–1214.

[5]Van Driest, E. R., "Turbulent Boundary Layers in Compressible Fluids," *Journal of the Aeronautical Sciences*, Vol. 18, March 1951, pp. 145–159.

[6]Oldenburg, R., Chinitz, W., Friedman, M., Jaffe, R., Jachimowski, C., Rabinowitz, M., and Schott, G., "Hypersonic Combustion Kinetics, Status Report of the Rate Constant Committee, NASP High-Speed Propulsion Technology Team," NASP TM 1107, May 1990.

[7]Anderson, G. Y., "SCRAM-A Program to Compute Supersonic Combustion Ramjet Performance," NASA Internal Rept., Hypersonic Propulsion Branch, April 9, 1968.